Manuscript submitted to Structural and Multidisciplinary Optimization

Sampling-based Probabilistic Analytical Target Cascading using Kernel Density Estimation for Accurate Uncertainty Propagation

Yongsu Jung

Department of Mechanical Engineering, Korea Advanced Institute of Science and Technology,

Daejeon, 34141, South Korea

Namwoo Kang

Department of Mechanical Systems Engineering, Sookmyung Women's University,

Seoul, 04310, South Korea

Ikjin Lee*

Department of Mechanical Engineering, Korea Advanced Institute of Science and Technology,

Daejeon, 34141, South Korea

Keywords: Multidisciplinary Design Optimization (MDO), Reliability-based Design Optimization (RBDO), Probabilistic Analytical Target Cascading (PATC), Uncertainty Propagation, Kernel Density Estimation (KDE)

* Corresponding author: ikjin.lee@kaist.ac.kr

Abstract

Probabilistic analytical target cascading (PATC) has been developed to incorporate uncertainty of random variables in a hierarchical multilevel system using the framework of ATC. In the decomposed ATC structure, consistency between linked subsystems has to be guaranteed through individual subsystem optimizations employing special coordination strategies such as augmented Lagrangian coordination. However, the consistency in PATC has to be treated exploiting uncertainty quantification and propagation of interrelated linking variables that is the major concern of PATC. In previous works, the consistency of linking variables is assured by matching statistical moments under the normality assumption. However, it can induce significant error when the linking variable to be quantified is highly nonlinear and non-normal. In addition, reliability computed from statistical moments may be inaccurate in each optimization of the subsystem. To tackle the challenges, we propose the sampling-based PATC using kernel density estimation (KDE). The framework of reliability-based design optimization (RBDO) using sampling methods is adopted in individual optimizations of subsystems in the presence of uncertainty. The uncertainty quantification of a linking variable which is an intermediate random response can be achieved by shifted KDE. The constructed KDE based on finite samples of the linking variable can provide statistical representations to linked subsystems, and it can be utilized in the sampling-based RBDO through random samplings at the current design point. For the proposed sampling-based PATC, stochastic sensitivity analysis for KDE is further developed. The proposed sampling-based PATC using KDE facilitates efficient and accurate procedures to obtain a system optimum in PATC, and two examples based on mathematical function and finite element analysis (FEA) are used to demonstrate effectiveness of the proposed approach.

1. Introduction

Generally, a large-scale complex system such as a vehicle and an airplane consists of multiple and hierarchical subsystems which are intricately linked with each other through variables and responses making it challenging to optimize the whole system at once due to its complexity. Therefore, decomposition-based optimization methods with special coordination between linked subsystems have been developed to optimize the large-scale complex system (Sobieszczanski and Haftka 1997; Alexandrov and Lewis 2002; Kokkolaras et al. 2004; Allison et al. 2009; Martins and Lambe 2013; Bayrak et al. 2016; Cho et al. 2016; Papalambros and Wilde 2017).

Analytical target cascading (ATC) is one of the decomposition-based methods where a system is partitioned into several hierarchical subsystems with targets and responses (Kim et al. 2003a, b, 2006; Michelena et al. 2003; Tosserams et al. 2006, 2008; Li et al. 2008; Han and Papalambros 2010; DorMohammadi and Rais-Rohani 2013; Kang et al. 2014a, b; Jung et al. 2018). In the early stage, ATC was specialized in hierarchical decomposition with multilevel subsystems, but later ATC with non-hierarchical decomposition was proposed as well (Tosserams et al. 2010). However, these researches were established based on deterministic optimization and thus may not find solutions for actual engineering applications influenced by various uncertainties. Therefore, it is obvious to take into account uncertainties propagated from subsystems, and uncertainty-based multidisciplinary design optimization (UMDO) was extensively reviewed in the literature (Yao et al. 2011). Probabilistic analytical target cascading (PATC) has been developed to treat the uncertainties in the framework of ATC (Kokkolaras et al. 2006; Liu et al. 2006, Xiong et al. 2010). Especially, PATC using moment-matching treats consistency of interrelated probabilistic characteristics (i.e., linking variable) and the probabilistic constraints using statistical moments such as mean and covariance. This approach is intuitive and straightforward, but can cause significant error when the propagated distribution is highly non-normal resulting in an unreliable system optimum. On the other hand, Ouyang et al. (2014) proposed sequential PATC (SPATC) which combines sequential optimization and reliability assessment (SORA) (Du and Chen 2004) and PATC to improve its efficiency by decoupling the

triple nested loop in PATC, and extended it to deal with mixed uncertainty including interval variables (Ouyang et al. 2018). However, reliability obtained from SORA is still inaccurate due to its approximations, and also MPP-based uncertainty analysis (MPPUA) (Du and Chen 2001), one of uncertainty propagation methods, is still inefficient for accurate statistical information. Several researches suggested more efficient and accurate PATC methods in various ways but without intrinsic modification in uncertainty propagation of linking variables. Distribution types for the linking variables have to be predetermined based on prior knowledge that is a major weakness of moment-matching since it can cause a significant error when an inappropriate distribution is assumed.

Therefore, the proposed research focuses on resolving accuracy issues existing in conventional PATC methods, especially PATC with moment-matching. For this purpose, a concrete framework called sampling-based PATC using uncertainty propagation specialized for linking variables is proposed. This allows each subsystem to be optimized more accurately under the scheme of the sampling-based RBDO and makes random linking variables consistent between subsystems. Thus, kernel density estimation (KDE) to transfer uncertainty of linking variables more accurately to corresponding subsystems and its stochastic sensitivity analysis to perform the sampling-based RBDO are developed in this study. Propagation and coordination for three types of design variables, which are local variables, coupling variables, and shared variables, are strictly defined depending on how it is manipulated as consistency constraints. Consequently, the sampling-based RBDO and augmented Lagrangian coordination and alternating direction method of multipliers (AL-AD) are successfully combined by applying KDE to connect both methodologies. In other words, individual optimizations of ATC are performed using the sampling-based RBDO to obtain an accurate optimum, and KDE connects individual optimizations to satisfy consistency constraints instead of moment-matching.

The article is organized as follows. Brief reviews including existing PATC and sampling-based RBDO are presented in Section 2. In Section 3, the proposed method is explained with key ideas of the new framework. Then, feasibility and effectiveness of the proposed framework are verified in Sections 4 and 5. Conclusion and future research are given in Section 6.

2. Overview of Conventional Analytical Target Cascading Methodologies

2.1 Non-hierarchical Analytical Target Cascading (ATC)

The proposed research is originated from the non-hierarchical ATC without a multilevel concept to treat more common structure in the real world (Tosserams et al. 2010). Parent-children subsystems defined under strict conditions with respect to linking variables are unnecessary in the non-hierarchical ATC. Readers can refer to the literature (Kim et al. 2003a, b; Tosserams et al. 2006) for detailed descriptions of hierarchical ATC. Any linked subsystem in the non-hierarchical ATC can communicate with other subsystems directly without any restriction. General structure describing the relationship between neighbors (i.e., linked subsystems) is illustrated in Figure 1. Optimization of a Subsystem *j* in the non-hierarchical ATC can be formulated as (Tosserams et al. 2010)

$$\begin{aligned} &\min_{\bar{\mathbf{x}}_j} f_j(\bar{\mathbf{x}}_j) + \sum_{n\in R_j} \pi(\mathbf{t}_{nj} - \mathbf{r}_{jn}) + \sum_{m\in T_j} \pi(\mathbf{t}_{jm} - \mathbf{r}_{mj}) \quad \text{where } \pi(\mathbf{c}) = \mathbf{v}^T\mathbf{c} + \left\|\mathbf{w}\circ\mathbf{c}\right\|_2^2 \\ &\text{subject to } \mathbf{g}_j(\bar{\mathbf{x}}_j) \le 0,\ \mathbf{h}_j(\bar{\mathbf{x}}_j) = 0 \\ &\text{with } \mathbf{r}_{jn} = \mathbf{S}_{jn}\mathbf{a}_j(\mathbf{x}_j, \mathbf{t}_{jm} \,|\, m\in T_j) \text{ for } n\in R_j,\ \bar{\mathbf{x}}_j = [\mathbf{x}_j, \mathbf{r}_{jn} \,|\, n\in R_j, \mathbf{t}_{jm} \,|\, m\in T_j] \end{aligned} \tag{1}$$

where $\bar{\mathbf{x}}_j$ represents the design variables for the Subsystem *j*, $\mathbf{x}_j$ represents the local design variables, $\mathbf{r}_{jn}$ represents the responses corresponding to the target $\mathbf{t}_{nj}$ from the Subsystem *n*. Similarly, $\mathbf{t}_{jm}$ represents the target corresponding to the response $\mathbf{r}_{mj}$ which is transferred from the Subsystem *m*. The functions f_j, $\mathbf{g}_j$, and $\mathbf{h}_j$ represent the local objective, inequality, and equality constraint functions, respectively. The function $\mathbf{a}_j$ is used to compute responses and $\mathbf{S}_{jn}$ is a binary selection matrix that selects components from $\mathbf{a}_j$. The $\circ$ symbol means a term-by-term multiplication of vectors. The augmented Lagrangian coordination is applied in Eq. (1) where $\mathbf{v}$ is the Lagrange multiplier vector and $\mathbf{w}$ is a penalty weight vector. It should be noted that both $\bar{\mathbf{x}}_j$ and $\mathbf{x}_j$ in Eq. (1) are deterministic design variables.

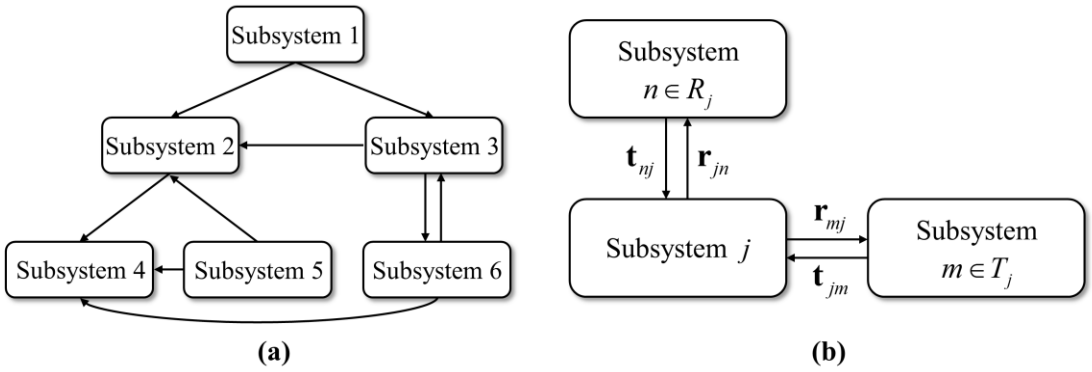

Fig. 1 (a) Functional dependence structure of non-hierarchical ATC and (b) Target and response flow between Subsystem *j* and its neighbors (modified from Tosserams et al. 2010)

2.2 Probabilistic Analytical Target Cascading (PATC) using Moment-matching

PATC using moment-matching combined with AL-AD can be formulated as (modified from Liu et al. 2006 and Tosserams et al. 2006)

$$
\begin{aligned}
&\text{Given } \boldsymbol{\mu}_{nj}, \boldsymbol{\sigma}_{nj}, \boldsymbol{\mu}_{mj}, \boldsymbol{\sigma}_{mj} \\
&\min_{\mu_{\bar{\mathbf{X}}_j}} f_j(\mu_{\bar{\mathbf{X}}_j}) + \sum_{n \in R_j} (\pi(\boldsymbol{\mu}_{nj} - \boldsymbol{\mu}_{jn}) + \pi(\boldsymbol{\sigma}_{nj} - \boldsymbol{\sigma}_{jn})) + \sum_{m \in T_j} (\pi(\boldsymbol{\mu}_{jm} - \boldsymbol{\mu}_{mj}) + \pi(\boldsymbol{\sigma}_{jm} - \boldsymbol{\sigma}_{mj})) \\
&\text{subject to } \mu_{\mathbf{g}_j} + k\sigma_{\mathbf{g}_j} \le \mathbf{0} \\
&\text{where } \pi(\mathbf{c}) = \mathbf{v}^{\mathrm{T}}\mathbf{c} + \left\| \mathbf{w} \circ \mathbf{c} \right\|_2^2 \qquad (2) \\
&\quad \mathbf{R}_{jn} = \mathbf{S}_{jn}\mathbf{a}_j(\mathbf{X}_j, \mathbf{T}_{jm} \,|\, m \in T_j) \text{ for } n \in R_j, \ \bar{\mathbf{X}}_j = [\mathbf{X}_j, \mathbf{R}_{jn} \,|\, n \in R_j, \mathbf{T}_{jm} \,|\, m \in T_j] \\
&\quad \boldsymbol{\mu}_{jn} = \mu(\mathbf{R}_{jn}), \ \boldsymbol{\sigma}_{jn} = \sigma(\mathbf{R}_{jn}) \\
&\quad \mathbf{T}_{jm} \sim N(\boldsymbol{\mu}_{jm}, \boldsymbol{\sigma}_{jm}^2)
\end{aligned}
$$

where $\bar{\mathbf{X}}_j$ is the random variable vector in the Subsystem *j*. Among the random design variables, $\mathbf{X}_j$ is the local design variable vector in the Subsystem *j* with known parametric distributions. Also, $\mathbf{T}_{jm}$ is assumed to follow a normal distribution for simplicity with the first two moments from the Subsystem *m*, which is denoted as $\boldsymbol{\mu}_{mj}$ and $\boldsymbol{\sigma}_{mj}$, respectively. In contrasts, $\mathbf{R}_{jn}$ is the probabilistic response to be computed in the Subsystem *j*, and statistical

moments are used in the consistency constraints. Also, the probabilistic constraints are estimated by the moment-matching method where k is constant corresponding to the given target reliability level.

The moment-matching method has two accuracy issues. First, the distributions of all matching quantities and constraints need to be close to the normal distribution in order for the method to be accurate. Second, the first two statistical moments should have a dominating impact on the optimum (Liu et al. 2006). However, these two conditions may not be always satisfied in real engineering applications.

2.3 Reliability Analysis and Sampling-based RBDO

Reliability analysis to consider the uncertainties can be categorized in general into analytical and sampling methods. The analytical methods have been developed using approximated performance functions (Breitung 1984; Tu et al. 1999; Adhikari 2004; Lee et al. 2008, 2012; Lim et al. 2014; Kang et al. 2017). On the other hands, the sampling methods mainly use random sampling in the probabilistic domain (Denny 2001; Rubinstein and Kroese 2016). So, design optimization using the sampling method for reliability analysis is called sampling-based reliability-based design optimization (RBDO) which is mainly employed in the paper due to its accuracy compared to the analytical methods (Lee et al. 2011a, b; Dubourg et al. 2011, 2013; Cho et al. 2014; Bae et al. 2018). Reliability analysis and stochastic sensitivity analysis are iteratively performed in the sampling-based RBDO to deal with probabilistic constraints. Unlike PATC using moment-matching which uses the first two moments of the subsystems, the proposed method applies the sampling-based RBDO to individual optimizations of the subsystems. In the sampling-based RBDO, the probability of failure can be computed as (Lee et al. 2011a, b)

$$\begin{aligned} P_F &\equiv P[G(\mathbf{X})>0] = \int I_{\Omega_F}(\mathbf{x})\, f_{\mathbf{X}}(\mathbf{x}) d\mathbf{x} = E(I_{\Omega_F}(\mathbf{x})) \\ \text{where } I_{\Omega_F}(\mathbf{x}) &= \begin{cases} 1, & \mathbf{x} \in \Omega_F \\ 0, & \text{otherwise} \end{cases} \\ \Omega_F &\equiv \{\mathbf{x} : G(\mathbf{x}) > 0\} \end{aligned} \tag{3}$$

where $P[\bullet]$ and $E[\bullet]$ represent a probability and an expectation measure, respectively; $G(\mathbf{x})$ is the constraint function; Ω_F is the failure set defined as $G(\mathbf{x})>0$; $f_{\mathbf{X}}(\mathbf{x})$ is the probability density function (PDF) of $\mathbf{X}$.

Moreover, sensitivity of the probability of failure is obtained through the stochastic sensitivity analysis with the first-order score function using PDFs of random design variables. Since the reliability analysis in Eq. (3) requires a large number of samplings, surrogate modeling is often employed in the sampling-based RBDO. Surrogate modeling methods and sampling strategies (Zhao et al. 2011; Chen et al. 2015; Liu et al. 2016) are beyond the scope of the paper. The paper will focus on how to construct an overall framework by connecting PATC and RBDO to alleviate the accuracy issues in the conventional PATC.

2.4 Kernel Density Estimation

Kernel density estimation (KDE) is a nonparametric way to estimate underlying PDF of a random variable based on sample points from the true but unknown distribution (Chen 2017; Silverman 2018) as the summation of kernel functions generated by the sample points. Thus, the estimated kernel density function can be expressed as

$$\hat{p}(x) = \frac{1}{nh}\sum_{i=1}^{n} k\left(\frac{X_i - x}{h}\right) \tag{4}$$

where n is the number of samples, $X_1, X_2, ..., X_n$ are independent, identically distributed random samples with density function p, $k(u)$ is the kernel function satisfying $\int_{-\infty}^{\infty} k(\mathrm{u})\,\mathrm{du} = 1$, and h is the positive smoothing parameter (i.e., bandwidth). It can be seen from Eq. (4) that the kernel function only depends on the smoothing parameter with the given samples. In this research, we use a second-order Gaussian kernel function which is the most popular kernel function. The smoothing parameter will be computed using the Rule-of-Thumb since the true distribution of a linking variable is unknown given by (Silverman 2018)

$$h = \left(\frac{4\hat{\sigma}^5}{3n}\right)^{\frac{1}{5}} \approx 1.06\hat{\sigma}n^{-\frac{1}{5}} \tag{5}$$

where $\hat{\sigma}^2$ is the sample variance and n is the number of samples. The Rule-of-Thumb assumed that the true distribution is close to the normal distribution, but it gives a plausible PDF for any true distribution. The detailed

description of KDE and methods to determine an optimal smoothing parameter to reduce mean integrated square error (MISE) can be seen in the literature (Chen 2017; Silverman 2018).

3. Sampling-based Probabilistic Analytical Target Cascading with Kernel Density Estimation

3.1 Terminology and Remarks

First, each variable and function for the proposed method have to be defined specifically and clearly. Assuming an extensive system with multiple subsystems, three types of variables can be classified in the decomposed subsystems: 1) local variables that belong to a single subsystem only, 2) coupling variables that behave as design variables in a subsystem and as responses in the corresponding subsystem, and 3) shared variables which are design variables in both linked subsystems. Coupling and shared variables are called linking variables. In order to prevent confusion in defining coupling variables, a coupling variable as a design variable is denoted as a coupling variable and a coupling variable as a response is denoted as a coupling response hereafter. Detailed notations to describe the proposed formulation are listed in Table 1 (Papalambros and Wilde 2017).

Table 1 Detailed description of notations in the proposed framework

Notation	Description
$\mathbf{X}_j^{Local}$	Random local variable in Subsystem *j*
$\mathbf{X}_{jn}^{Shared} \equiv \mathbf{X}_{nj}^{Shared}$	Random shared variable between Subsystem *j* and Subsystem *n*
$\mathbf{X}_{jn}^{Coup} \equiv \mathbf{Y}_{nj}^{Coup}$	Random coupling variable in Subsystem *j* and coupling response in Subsystem *n*
$\mathbf{Y}_{jn}^{Coup} \equiv \mathbf{X}_{nj}^{Coup}$	Random coupling response in Subsystem *j* and coupling variable in Subsystem *n*
$\mathbf{y}_{nj}^{Coup}$	Realization of $\mathbf{Y}_{nj}^{Coup}$ received from Subsystem *n*
$\bar{\mathbf{X}}_j = \{\mathbf{X}_j^{Local}, \mathbf{X}_{jn}^{Coup}, \mathbf{X}_{jn}^{Shared}\}$	Random design variable in Subsystem *j*
$\zeta(\mu, \sigma^2)$	Two-parameter distribution
$\hat{p}(x^{Coup}; s, \mathbf{y})$	Kernel density estimation with respect to shifting parameter *s* and sample $\mathbf{y}$
$\hat{\mathbf{R}}_{jn}$	Approximated response function to compute coupling response $\mathbf{Y}_{jn}^{Coup}$ in Subsystem *j*
$\hat{\mathbf{G}}_j$	Approximated performance function for constraints in Subsystem *j*

$\mathbf{P}_{j,\text{target}}$	Target probability of failure in Subsystem *j*
v	Lagrange multiplier
w	Penalty weight
$f_j(\mu_{\bar{\mathbf{x}}_j})$	Local objective function in Subsystem *j*

On the other hand, the coordination algorithm of ATC can be divided into the inner loop and the outer loop to achieve convergence and consistency of the system optimum. In the inner loop, individual optimizations of the subsystem are conducted in the presence of given parameters without any communication. In the outer loop, Lagrange multipliers and penalty weights are updated, and linking variables are transferred. In the perspective of the double-loop scheme, the sampling-based RBDO and surrogate modeling are performed in the inner loop of ATC, and uncertainty propagation is performed in the outer loop since uncertainties of linking variables will be propagated after RBDOs of all subsystems.

3.2 Basic Formulation for Sampling-based PATC: Inner Loop

3.2.1 Formulation

In this section, sampling-based RBDO of a general subsystem and how to establish consistency constraints between linking variables are explained. The proposed optimization formulation of a subsystem with three kinds of consistency constraints can be expressed as

$$
\begin{aligned}
&\text{Given } \mathbf{y}_{nj}^{Coup}, \boldsymbol{\mu}_{\mathbf{X}_{nj}^{Coup}}, \boldsymbol{\mu}_{\mathbf{X}_{nj}^{Shared}} \\
&\text{Find } \mu_{\bar{\mathbf{X}}_j} = \{\boldsymbol{\mu}_{\mathbf{X}_{jn}^{Local}}, \boldsymbol{\mu}_{\mathbf{X}_{jn}^{Coup}}, \boldsymbol{\mu}_{\mathbf{X}_{jn}^{Shared}}\} \\
&\min_{\mu_{\bar{\mathbf{X}}_j}} f_j(\mu_{\bar{\mathbf{X}}_j}) + \sum_{n \in R_j} \pi(\mu(\mathbf{y}_{nj}^{Coup}) - \boldsymbol{\mu}_{\mathbf{X}_{jn}^{Coup}}) + \pi(\boldsymbol{\mu}_{\mathbf{X}_{nj}^{Coup}} - \mu(\mathbf{Y}_{jn}^{Coup})) + \pi(\boldsymbol{\mu}_{\mathbf{X}_{nj}^{Shared}} - \boldsymbol{\mu}_{\mathbf{X}_{jn}^{Shared}}) \\
&\text{subject to } \Pr(\hat{\mathbf{G}}_j(\bar{\mathbf{X}}_j) \le 0) \le \mathbf{P}_{j,\text{target}} \\
&\text{where } \pi(\mathbf{c}) = \mathbf{v}^{\mathrm{T}}\mathbf{c} + \left\|\mathbf{w} \circ \mathbf{c}\right\|_2^2 \qquad (6) \\
&\bar{\mathbf{X}}_j = [\mathbf{X}_j^{Local}, \mathbf{X}_{jn}^{Coup}, \mathbf{X}_{jn}^{Shared}], \quad \mathbf{Y}_{jn}^{Coup} = \hat{\mathbf{R}}_{jn}(\bar{\mathbf{X}}_j) \\
&\mathbf{X}_j^{Local} \sim \zeta_j^{Local}(\boldsymbol{\mu}_{\mathbf{X}_j^{Local}}, \boldsymbol{\sigma}^2_{\mathbf{X}_j^{Local}}) \\
&\mathbf{X}_{jn}^{Shared} \sim \zeta_{jn}^{Shared}(\boldsymbol{\mu}_{\mathbf{X}_{jn}^{Shared}}, \boldsymbol{\sigma}^2_{\mathbf{X}_{jn}^{Shared}}) \\
&\mathbf{X}_{jn}^{Coup} \sim \hat{p}(\mathbf{x}_{jn}^{Coup}; \boldsymbol{\mu}_{\mathbf{X}_{jn}^{Coup}}, \mathbf{y}_{nj}^{Coup})
\end{aligned}
$$

where ζ means any parametric distribution with two parameters, $\hat{p}$ is shifting kernel density estimation, $\hat{\mathbf{G}}_j$ and $\hat{\mathbf{R}}_j$ are Kriging surrogate models to approximate expensive performance function $\mathbf{G}_j$ and coupling response $\mathbf{Y}_{jn}^{Coup}$ in subproblem *j*, respectively. The probabilistic constraints are evaluated using Eq. (3), and the augmented Lagrangian coordination is used in the formulation to reduce inconsistency between linking variables.

The objective function in Eq. (6) includes a penalty function regarding three types of consistency constraints. First, $\pi(\mu(\mathbf{y}_{nj}^{Coup}) - \boldsymbol{\mu}_{\mathbf{X}_{jn}^{Coup}})$ is associated with a coupling variable in Subsystem *j* and a coupling response in Subsystem *n*. $\mu(\mathbf{y}_{nj}^{Coup})$ is the sample mean of $\mathbf{y}_{nj}^{Coup}$ which is the realization of the random coupling response received from the Subsystem *n*, and $\boldsymbol{\mu}_{\mathbf{X}_{jn}^{Coup}}$ is the shifted mean using KDE based on $\mathbf{y}_{nj}^{Coup}$. The second term $\pi(\boldsymbol{\mu}_{\mathbf{X}_{nj}^{Coup}} - \mu(\mathbf{Y}_{jn}^{Coup}))$ also corresponds to a coupling variable in an opposite way. It is a coupling variable in Subsystem *n* and a coupling response in Subsystem *j*. The third term $\pi(\boldsymbol{\mu}_{\mathbf{X}_{nj}^{Shared}} - \boldsymbol{\mu}_{\mathbf{X}_{jn}^{Shared}})$ is related to a shared variable. Because distribution of the shared variable is known, uncertainty propagation using KDE is not necessary. Only the design point which is the mean is used in the consistency constraint.

3.2.2 Subsystem Composition

Detailed composition of a general subsystem is illustrated in a single subsystem in Figure 2 where subscripts concerning the subsystem are omitted. A vector of local variables is denoted as $\mathbf{X}^{Local}$ which contains all random local variables. A vector of shared variables is denoted as $\mathbf{X}^{Shared}$ imposed to be consistent with linked subsystems. A vector of coupling variables is denoted as $\mathbf{X}^{Coup}$. Since it is not a design variable in the system-level, variability of $\mathbf{X}^{Coup}$ should be assigned by the corresponding subsystem as a coupling response through KDE. On the other hands, responses to be computed in the subsystem can be categorized into performance functions and coupling responses. The performance function $\mathbf{G}^{Perf}$ is involved in probabilistic constraints for the optimization, and the coupling response $\mathbf{Y}^{Coup}$ is computed to propagate uncertainty.

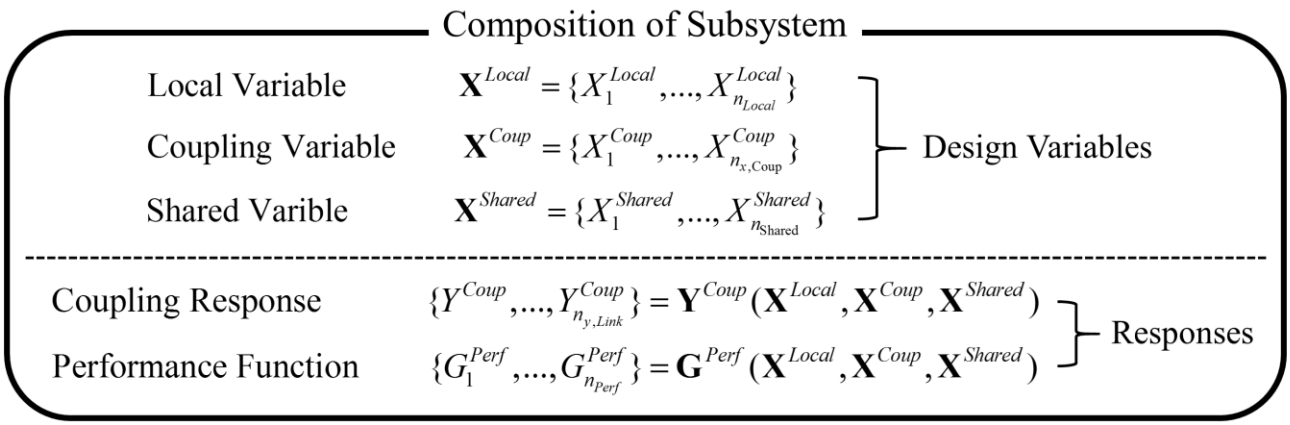

Fig. 2 Composition of a general subsystem

Figure 3 shows a simple example with three subsystems. Each subsystem has own local variables, and there are two coupling variables and one shared variable. The arrow between two subsystem means the consistency constraint. Subsystems 1 and 2 are linked with a coupling variable. The coupling response in Subsystem 2 is propagated to Subsystem 1 with the distribution in red, and Subsystem 1 is optimized with the propagated

variability of Y_{21}^{Coup} returning $\mu_{X_{12}^{Coup}}$ to Subsystem 2. Therefore, the consistency constraint can be expressed as $\mu_{X_{12}^{Coup}} - \mu(Y_{21}^{Coup})$. Identical explanation can be applied for the relationship between Subsystems 1 and 3 with the distribution in blue. On the other hand, Subsystems 2 and 3 are linked with a shared variable only whose distribution is already known. Hence, its mean is transferred which means the consistency constraint is denoted as $\mu_{X_{23}^{Shared}} - \mu_{X_{32}^{Shared}}$.

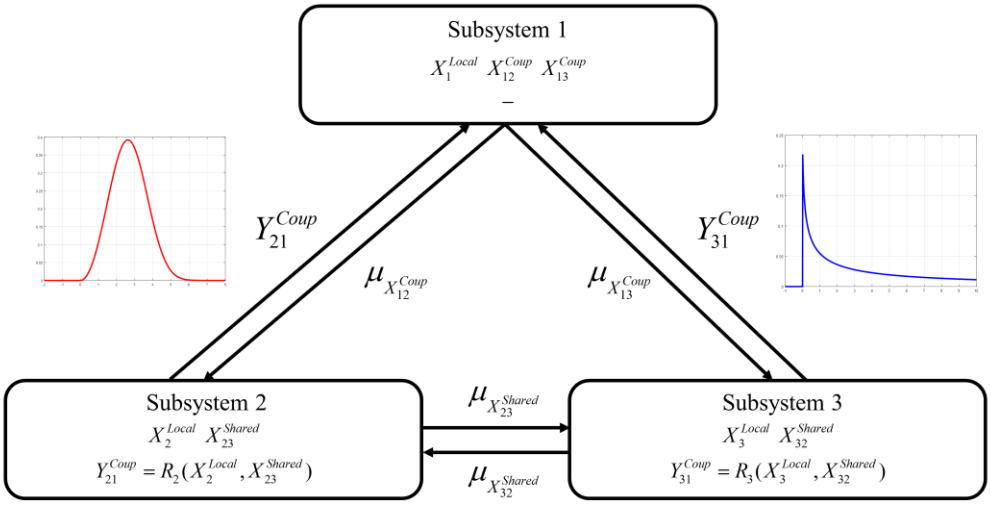

Fig. 3 Flow of linking variables between linked subsystems

3.2.3 Surrogate Modeling

Surrogate modeling is utilized in the proposed PATC framework especially in the inner loop to alleviate expensive computational cost. For further efficiency improvement, sequential sampling strategies are oftern combined with surrogate modeling. The constraint boundary sampling (CBS) is adapted in this study to enhance accuracy and efficiency of surrogate models. The CBS criterion is formulated as (Lee and Jung 2008)

$$CBS = \begin{cases} \sum_{i=1}^{N} \phi\left(\frac{\hat{g}_i(x)}{\sqrt{MSE_i}}\right) \cdot D & \text{if } \hat{g}_i(x) \geq 0, \forall i \\ 0 & \text{otherwise} \end{cases} \quad (7)$$

where D is the minimal distance from the current sample point to the existing sample points and $\hat{g}_i(x)$ is the mean of the Kriging model at the current point x and MSE_i indicates the variance of the current sample point. For further improvement in efficiency, the local window concept with CBS has been employed (Chen et al. 2014).

One important thing to be discussed when using surrogate models is that the design space can be partitioned in the ATC structure. This means that high-dimensional design space can be decomposed into several low-dimensional design spaces, and unlike existing ATC, it may be efficient than even All-in-One (AiO) which optimizes the entire system at once in the high-dimensional design space since the number of samplings to achieve acceptable level of accurcay increases exponentially with dimensions, called "the curse of dimensionality". Efficiency comparison with AiO is beyond the scope of the paper, so we will use it for reference only.

3.3 Uncertainty Propagation and Sensitivity Analysis for Kernel Density Estimation: Outer Loop

3.3.1 Shifted Kernel Density Estimation

In the outer loop of the proposed PATC, mean vectors including local, shared, and coupling variables and nonparametric distributions of coupling responses have to be exchanged, and the corresponding Lagrange multipliers and penalty weights are appropriately updated using AL-AD. Even though the sampling-based RBDO can be adapted into the optimization of individual subsystems, ATC structure always has linking variables transferred from linked subsystems. Therefore, the uncertainty propagation of the linking variable, the key concept of the proposed framework, have to be developed preferentially. This section introduces how to propagate uncertainties of coupling variables.

A coupling variable is not a random design variable in the system-level but an intermediate response due to decomposition which is a function of design variables. Therefore, uncertainty quantification of a coupling variable is indispensable for reliability analysis and consistency constraints; however, explicit expression of its uncertainty cannot be achieved. In the proposed method, uncertainty quantification and propagation of a coupling variable are conducted using KDE. KDE with a set of given samples can represent a nonparametric distribution as

$$\hat{p}_j(x; y_{j,i}^{Coup}) = \frac{1}{nh}\sum_{i=1}^{n} k(\frac{y_{j,i}^{Coup} - x}{h})$$
$$\text{where } k(u) = \frac{1}{\sqrt{2\pi}}\exp(-\frac{1}{2}u^2) \quad (8)$$
$$y_{j,i}^{Coup} = R_j(\overline{\mathrm{x}}_i) \quad \text{for } i = 1,2,...,n$$

where $\hat{p}_j(x)$ is the estimated PDF of the coupling response $R_j(\overline{\mathbf{x}})$ computed in the corresponding subsystem, and *n* is the number of samples. If the coupling variable has to estimate PDF from a linked subsystem as Eq. (8), it should be shifted based on the current design point. It means that statistical characteristics of the coupling response are maintained except for the design point (i.e., mean). In consequence, the PDF of a coupling variable through KDE and a shifting parameter can be expressed as

$$X_j^{Coup} \sim \hat{p}_j(x; s(y_i^{Coup}, \mu_{x_j^{Coup}}), \mathbf{y}^{Coup}) = \frac{1}{nh}\sum_{i=1}^{n} k(\frac{s(y_{j,i}^{Coup}, \mu_{x_j^{Coup}}) - x}{h}) \quad (9)$$
$$\text{where } s(y_{j,i}^{Coup}, \mu_{x_j^{Coup}}) = y_{j,i}^{Coup} - \mu(\mathbf{y}_j^{Coup}) + \mu_{x_j^{Coup}}$$

where $y_{j,i}^{Coup}$ is the *i*-th realization of the *j*-th coupling response from the linked subsystem, $\mu(\mathbf{y}^{Coup})$ is the mean of $\mathbf{y}_{j,i}^{Coup} = \{y_{j,1}^{Coup}, y_{j,2}^{Coup}, ...y_{j,n}^{Coup}\}$, and $\mu_{x_j^{Coup}}$ is the design point of a corrsponding coupling variable. Through the shifting of the samples, only the numerical expectation of KDE is changed (Silverman 2018). In the proposed method, the consistency constraint can be arranged with the mean, but uncertainties are transferred as a nonparametric distribution without loss of any statistical information unlike PATC using moment-matching.

3.3.2 Sensitivity Analysis for Kernel Density Estimation

To perform sampling-based RBDO in the proposed PATC, stochastic sensitivity for probabilistic constraints with respect to random design variables needs to be estimated accurately. When distributions of random design variables are known, stochastic sensitivities using the first-order score function with respect to the mean are obtained even if input random variables are correlated (Lee et al. 2011a, b; Cho et al. 2016). However, since

KDE is used in the proposed PATC to approximate PDFs of coupling variables, analytical sensitivity analysis for KDE is derived in this section and its accuracy is verified using the finite difference method (FDM) in Section 4.

Sensitivity of probability of failure with respect to the mean of the independent random variable including local and shared variables whose distributions are known is obtained as

$$\begin{aligned}\frac{\partial P_F(\boldsymbol{\mu})}{\partial \mu} &= \frac{\partial}{\partial \mu}\int I_{\Omega_F}(\mathbf{x}) f_{\mathbf{X}}(\mathbf{x};\boldsymbol{\mu})\,\mathrm{d}\mathbf{x} \\ &= \int I_{\Omega_F}(\mathbf{x})\frac{\partial f_{\mathbf{X}}(\mathbf{x};\boldsymbol{\mu})}{\partial \mu}\,\mathrm{d}\mathbf{x} \\ &= \int I_{\Omega_F}(\mathbf{x})\frac{\partial \ln f_{\mathbf{X}}(\mathbf{x};\boldsymbol{\mu})}{\partial \mu} f_{\mathbf{X}}(\mathbf{x};\boldsymbol{\mu})\,\mathrm{d}\mathbf{x} \\ &= E[I_{\Omega_F}(\mathbf{x})\frac{\partial \ln f_{\mathbf{X}}(\mathbf{x};\boldsymbol{\mu})}{\partial \mu}] \\ \text{where } \mathrm{s}_{\mu}^{(1)} &\equiv \frac{\partial \ln f_{\mathbf{X}}(\mathbf{x};\boldsymbol{\mu})}{\partial \mu} \\ \mathbf{X} &= \{\mathbf{X}^{Local}, \mathbf{X}^{Shared}\}\end{aligned} \tag{10}$$

where $\mathrm{s}_{\mu}^{(1)}$ is the first-order score function for mean (Lee et al. 2011b) and directly obtained from the known input distributions. In case of independent coupling variables, the first-order score function of KDE with respect to mean can be derived as

$$\begin{aligned}\frac{\partial \ln f_{\mathbf{X}}(\mathbf{x};\boldsymbol{\mu})}{\partial \mu} &\equiv \frac{\partial \ln \hat{p}_h(\mathbf{x};\mathbf{h})}{\partial \mu} \\ &= \frac{\partial \ln \hat{p}_h}{\partial x_1}\frac{\partial x_1}{\partial \mu} + \frac{\partial \ln \hat{p}_h}{\partial x_2}\frac{\partial x_2}{\partial \mu} + \ldots + \frac{\partial \ln \hat{p}_h}{\partial x_n}\frac{\partial x_n}{\partial \mu} \\ &= \sum_{i=1}^{n}\frac{x - x_i}{\sqrt{2\pi} n h^3 \hat{p}_h(x)} e^{-\frac{1}{2}(\frac{x-x_i}{h})^2} \\ \text{where } \hat{p}_h(x) &= \frac{1}{nh}\sum_{i=1}^{n}\phi(\frac{x-x_i}{h}) = \frac{1}{nh}(\frac{1}{\sqrt{2\pi}} e^{-\frac{1}{2}(\frac{x-x_1}{h})^2} + \ldots + \frac{1}{\sqrt{2\pi}} e^{-\frac{1}{2}(\frac{x-x_n}{h})^2}) \\ \mu &= \frac{x_1 + x_2 + \ldots + x_n}{n} \\ \mathbf{x} &= \{x_1, x_2, \ldots, x_n\} = \{\mathbf{y}^{Coup} - \mu(\mathbf{y}^{Coup}) + \mu_{x_j^{Coup}}\} \\ \frac{\partial \mathbf{x}}{\partial \mu} &= \mathbf{1}\end{aligned} \tag{11}$$

where $\mathbf{x}$ is the shifted samples of a coupling response, and h is the smoothing parameter obtained using Eq. (5). It is noted that all data are shifted simultaneously meaning that the partial derivative with respect to the mean is one. Plugging the first-order score function of KDE with respect to independent random variables in Eq. (11) into Eq. (10) yields sensitivity of probability of failure for coupling variables.

3.4 Flowchart of Methodology

This section explains the proposed algorithm in detail using a flowchart and conceptional system framework. Figure 4 describes the overall flowchart of the proposed PATC. First, deterministic optimizations of individual subsystems updating Kriging models have to be performed iteratively while the Lagrange multipliers and the penalty weights are updated using AL-AD. Once the deterministic ATC successfully converges to the optimum, it becomes the initial point of the sampling-based PATC.

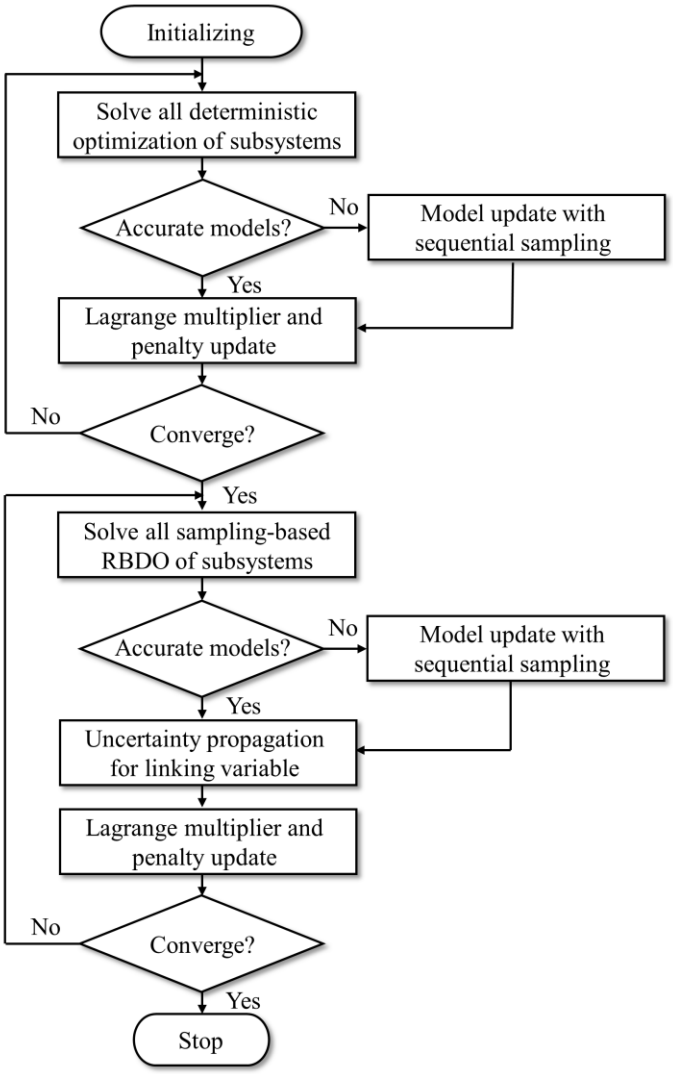

Fig. 4 Overall flowchart of the proposed PATC

Figure 5 shows a conceptional system framework of a vehicle example using a three-subsystem model with own finite element analysis (FEA) model for performance computation. Subsystem 1 for the vehicle body model is influenced by Subsystems 2 and 3 for the vehicle component models because Subsystems 2 and 3 have coupling responses which are coupling variables in Subsystem 1. It is shown that FEA is performed only on the specific sampling points, and the sampling-based RBDO is performed using the Kriging models. Especially, the linking

variable is propagated to Subsystem 1 through KDE, and then reliability analysis and sensitivity analysis will be carried out iteratively.

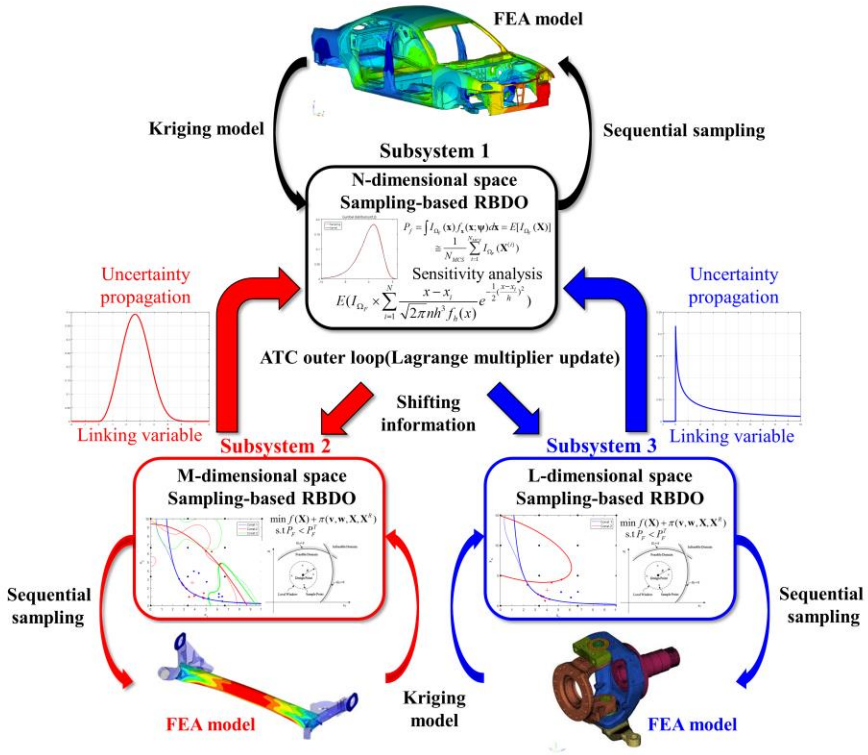

Fig. 5 System framework of the proposed methodology (reproduced from Altair Hyperworks)

It is shown that three subsystems have divided dimensions such as N, M, and L in Figure 5. As mentioned in Section 3.2, if these three subsystems combine into a single system, the total dimension is definitely less than N+M+L due to the duplicated linking variables. However, the number of sampling points in single high-dimensional space for satisfying acceptable accuracy may be larger than several low-dimensional design spaces. For instance, when a 15-dimensional system may be decomposed into four 5-dimensional subsystems, the number of samplings to construct the surrogate model on 15-dimensional design space is expected to be much larger than decomposed 5-dimensional design spaces. This could be one application of the proposed PATC to improve efficiency of high dimensional large-scale design optimization problems.

4. Numerical Example: Three-dimensional Mathematical Example

A three-dimensional mathematical example is employed to demonstrate feasibility of the developed framework compared to AiO and PATC using moment-matching in terms of accuracy and efficiency. In addition, the proposed sensitivity analysis for KDE is compared with FDM. It is expected that the proposed framework shows comparable efficiency in the decomposed low-dimensional subspaces than the high-dimensional AiO space and high accuracy through the uncertainty propagation of nonparametric distributions without any loss of information unlike the moment-matching method.

4.1 Formulation of Three-dimensional Mathematical Example

RBDO with the three-dimensional system is written as

$$
\begin{aligned}
\min \quad & f_1(\mu_{\mathbf{X}}) + f_2(\mu_{\mathbf{X}}) \\
\text{s.t} \quad & \Pr[G_i(\mathbf{X}) > 0] \le 0.05 \quad \text{for i =1,...,5} \\
\text{where} \quad & f_1(\mu_{\mathbf{X}}) = -\frac{(\mu_{X_1} + \mu_{X_2} - 10)^2}{30} - \frac{(\mu_{X_1} - \mu_{X_2} + 10)^2}{120},\ f_2(\mu_{\mathbf{X}}) = \mu_{X_3} + \frac{\mu_{2X_1^2 - X_2}}{10} \\
& G_1(\mathbf{X}) = 1 - \frac{X_1^2 X_2}{20} \\
& G_2(\mathbf{X}) = -1 + (0.9063X_1 + 0.4226X_2 - 6)^2 + (0.9063X_1 + 0.4226X_2 - 6)^3 - \\
& \qquad 0.6(0.9063X_1 + 0.4226X_2 - 6)^3 - (-0.4226X_1 + 0.9063X_2) \\
& G_3(\mathbf{X}) = 1 - \frac{80}{X_1^2 + 8X_2 + 5},\ G_4(\mathbf{X}) = 1 - \frac{X_3^2}{20} \times \frac{2X_1^2 - X_2}{10} \\
& G_5(\mathbf{X}) = 1 - \frac{(X_3 + \frac{2X_1^2 - X_2}{10} - 10)^2}{30} - \frac{(X_3 - \frac{2X_1^2 - X_2}{10} + 10)^2}{120} \\
& X_i \sim N(\mu_{X_i}, 0.5^2) \quad \text{for } i = 1,2,3
\end{aligned}
\tag{12}
$$

where three random design variables follow the normal distribution and the target probability of failure is set to 5% in all constraints. Generally, ATC assumes that Eq. (12) is a system optimization which cannot be solved in AiO strategy. Thus, Eq. (12) is used to validate the system optimum and compare computational cost with the proposed PATC.

4.2 Formulation of Decomposed Three-dimensional Mathematical Example

The decomposed structure through the proposed framework is described in Figure 6 which show three types of design variables and two types of responses. There is no shared variable, and Subsystem 1 has a coupling response, and Subsystem 2 has the corresponding coupling variable. There is one consistency constraint with respect to the coupling variable vanished in the system-level optimization in Eq. (12).

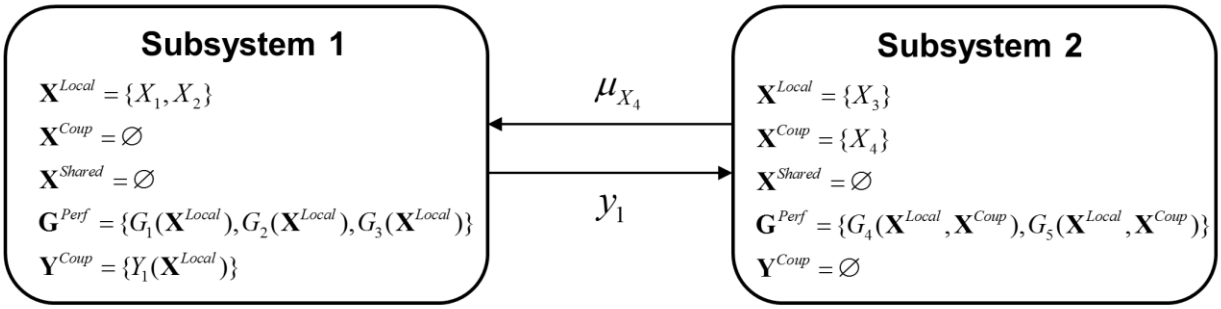

Fig. 6 Structure of decomposed subsystems

The optimization of Subsystem 1 is formulated as

$$
\begin{aligned}
&\min_{\mu_{X_1}, \mu_{X_2}} \quad -\frac{(\mu_{X_1} + \mu_{X_2} - 10)^2}{30} - \frac{(\mu_{X_1} - \mu_{X_2} + 10)^2}{120} + \pi(\mu(\mathbf{y}_1) - \mu_{X_4}) \\
&\text{s.t} \quad \Pr[G_i(\mathbf{X}) > 0] \le 0.05 \quad \text{for i =1,2,3} \\
&\text{where} \quad G_1(\mathbf{X}) = 1 - \frac{X_1^2 X_2}{20} \\
&\qquad G_2(\mathbf{X}) = -1 + (0.9063X_1 + 0.4226X_2 - 6)^2 + (0.9063X_1 + 0.4226X_2 - 6)^3 - \\
&\qquad\qquad 0.6(0.9063X_1 + 0.4226X_2 - 6)^3 - (-0.4226X_1 + 0.9063X_2) \\
&\qquad G_3(\mathbf{X}) = 1 - \frac{80}{X_1^2 + 8X_2 + 5} \\
&\qquad Y_1(X_1, X_2) = \frac{2X_1^2 - X_2}{10} \\
&\qquad X_1 \sim N(\mu_{X_1}, 0.5^2) \\
&\qquad X_2 \sim N(\mu_{X_2}, 0.5^2) \\
&\qquad \mathbf{X}^{Local} = \{X_1, X_2\},\ \mathbf{X}^{Coup} = \varnothing,\ \mathbf{X}^{Shared} = \varnothing,\ \mathbf{Y}^{Coup} = \{Y_1\}
\end{aligned}
\tag{13}
$$

where $Y_1(X_1, X_2)$ is the coupling response to be transferred to Subsystem 2. The consistency constraint using $\mu(\mathrm{Y}_1)$ and μ_{X_4} is combined into the objective function as a penalty function. Only local variables are random design variables in Subsystem 1.

Similarly, the optimization of Subsystem 2 is formulated as

$$
\begin{aligned}
&\min_{\mu_{\mathrm{X}_3}, \mu_{\mathrm{X}_4}} \quad \mu_{\mathrm{X}_3} + \mu_{\mathrm{X}_4} + \pi(\mu(\mathbf{y}_1) - \mu_{\mathrm{X}_4}) \\
&\text{s.t} \quad \Pr[G_i(\mathbf{X}) > 0] \le 0.05 \quad \text{for i =4,5} \\
&\text{where} \quad G_4(\mathbf{X}) = 1 - \frac{X_3^2 X_4}{20} \\
&\qquad G_5(\mathbf{X}) = 1 - \frac{(X_3 + X_4 - 10)^2}{30} - \frac{(X_3 - X_4 + 10)^2}{120} \\
&\qquad X_3 \sim N(\mu_{\mathrm{X}_3}, 0.5^2) \\
&\qquad X_4 \sim \hat{p}_4(x) = \frac{1}{nh} \sum_{i=1}^{n} k\left(\frac{s(y_i, \mu_{\mathrm{X}_4}) - x}{h}\right) \text{ for } s(y_i) = y_i - \mu(\mathbf{y}_1) + \mu_{\mathrm{X}_4} \\
&\qquad \mathbf{X}^{Local} = \{X_3\}, \ \mathbf{X}^{Coup} = \{X_4\}, \ \mathbf{X}^{Shared} = \varnothing, \ \mathbf{Y}^{Coup} = \varnothing
\end{aligned}
\tag{14}
$$

where X_4 is the coupling variable propagated from Subsystem 1 and its uncertainty is described with the shifted KDE explained in Section 3.3.1. There are two random design variables which are a local variable and coupling variable with no coupling response, and other properties are analogous with Subsystem 1. It is noted that Subsystems 1 and 2 can be combined with substitution of the coupling response $Y_1(X_1, X_2)$ as a function of design variables.

4.3 Validation of Sensitivity Analysis for Kernel Density Estimation

In this section, accuracy of the proposed sensitivity analysis is compared with numerical sensitivity analysis using G_1 and G_2 in Eq. (12). Variability of X_1 is quantified by KDE with 50 samples drawn from the known parametric distribution, and X_2 is assumed to follow a normal distribution. Comparison tests are performed by varying the true distribution of X_1 such as Normal, Lognormal, and Gumbel distributions, and the results are compared to FDM with various perturbations such as 1.0%, 0.5%, and 0.1%. The number of samples drawn from

KDE and the normal distribution to compute the probability of failure is 10^7 at two different design points which are $\mathbf{d}_1 = [4.56, 1.86]^T$ and $\mathbf{d}_2 = [4.32, 1.95]^T$ with $\sigma = 0.5$ for both random variables.

Table 2 shows the results of the proposed and numerical sensitivity analysis for G_1 and G_2 in Eq. (12). Discrepancies between two sensitivity analysis results in case of 0.1% perturbation are also shown in parenthesis. The numerical sensitivity analysis is performed using fixed random seed to eliminate sampling uncertainty, and the proposed method shows accurate results regardless of the true distribution type or design point location.

Table 2 Results of sensitivity analysis with numerical and analytical methods

True Distribution of X_1	Design Sensitivity	G_1 at $\mathbf{d}_1$	G_2 at $\mathbf{d}_1$	G_1 at $\mathbf{d}_2$	G_2 at $\mathbf{d}_2$
Normal	FDM (1.0%)	-0.0975	0.0823	-0.1287	0.0275
	FDM (0.5%)	-0.1006	0.0798	-0.1314	0.0264
	FDM (0.1%)	-0.1027	0.0774	-0.1346	0.0249
	Proposed	-0.1020 (0.68%)	0.0764 (1.30%)	-0.1351 (0.37%)	0.0250 (0.40%)
Lognormal	FDM (1.0%)	-0.0987	0.0768	-0.1305	0.0291
	FDM (0.5%)	-0.1012	0.0742	-0.1340	0.0278
	FDM (0.1%)	-0.1037	0.0724	-0.1395	0.0272
	Proposed	-0.1026 (1.07%)	0.0721 (0.41%)	-0.1365 (2.19%)	0.0270 (0.74%)
Gumbel	FDM (1.0%)	-0.0951	0.0784	-0.1338	0.0339
	FDM (0.5%)	-0.0975	0.0761	-0.1370	0.0333
	FDM (0.1%)	-0.1012	0.0752	-0.1381	0.0330
	Proposed	-0.1001 (1.09%)	0.0727 (3.43%)	-0.1401 (1.42%)	0.0322 (2.58%)

4.4 Results of Sampling-based PATC

AiO sampling-based RBDO results using Eq. (12) are listed in Table 3. Initial samples are obtained by the grid sampling on the whole design space with different levels, and the number of sequential samplings means additional samples during the optimization. There are five constraints among which only three are active. The probability of failure computed from the exact functions is written in the last column for each case. Definitely, AiO shows high accuracy, but requires a number of sequential samplings regardless of the number of the initial samples.

Table 3 Required samples and optimums obtained from AiO with different initial sampling

Initial grid samples	Additional samples	Optimum	Probability of failure (%)
125 (5-level)	50	$\{3.7549, 2.6423, 4.0267\}^T$	[5.00, 5.01, 4.98]
64 (4-level)	48	$\{3.7541, 2.6461, 4.0309\}^T$	[4.96, 4.97, 5.03]
27 (3-level)	51	$\{3.7539, 2.6446, 4.0281\}^T$	[4.99, 5.00, 4.99]

As mentioned before, the proposed method uses the optimum of deterministic ATC as the initial design. In each 2D subsystem, grid sampling with 5-level full factorial design is adopted to generate initial samples, which means that 25 samples are used to construct initial Kriging models for the constraints and coupling response as shown in Figure 7. The solid and dotted lines in the figure mean the true and approximated limit-state functions by the Kriging model using 25 grid samples marked as black solid circles, respectively.

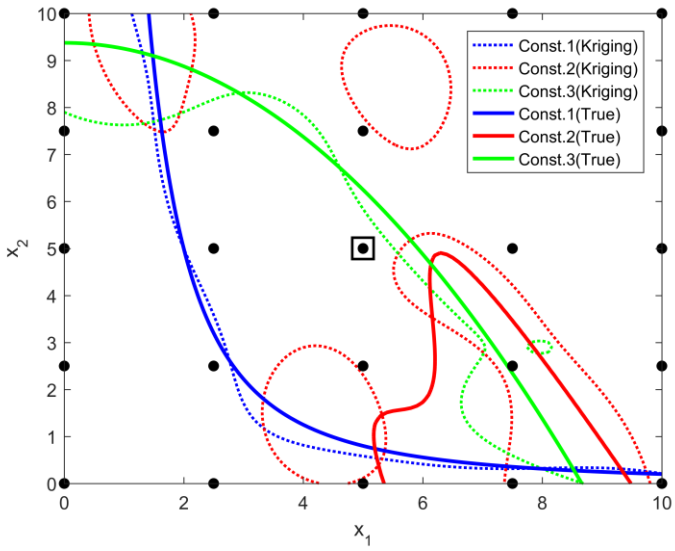

Fig. 7 True and approximated limit-state functions in Subsystem 1

Using the approximated limit-state functions in Figure 7, the proposed PATC is performed based on the algorithm in Figure 4. The tolerance for convergence is set to 5×10^{-3}, the number of MCS samples is 5×10^{5}, and the number of samples for the stochastic sensitivity proposed in Section 3.3.2 is 10^{4}. All initial Lagrange

multipliers and penalty weights are set to 1 and 0, respectively. A fixed local window whose radius is $0.3\beta_t$ for deterministic ATC and $1.6\beta_t$ for PATC is used for simplicity.

Figure 8 illustrates additional samples, updated Kriging model as dotted lines, and the design point in Subsystem 1 at the end of each process of ATC and sampling-based PATC. It is shown from the figure that the additional samples are located in the vicinity of the limit-state functions. Table 4 shows optimization results of the proposed method. From Tables 3&4, it can be seen that the optimum from the proposed PATC is very close to the ones by AiO, and the number of total samples for the proposed PATC is less than AiO in the 5-level grid sampling case. From Table 5 which shows optimization results by PATC using moment-matching, it can be seen that probability of failure at the optimum is inaccurate due to the normality assumption on the coupling variable compared with the proposed method. It is noted that only mean is used to construct the consistency constraint since the standard deviation goes to zero during PATC using moment-matching. Therefore, the standard deviation is merely given from Subsystem 1. Figure 9 shows difference between two methods in estimation of distribution of the coupling variable. The difference is because PATC using moment-matching assumes the distribution as a normal distribution with estimated mean and variance, whereas the proposed PATC estimates the distribution using KDE. Moreover, the difference will be larger as non-normality of the coupling variable is much larger.

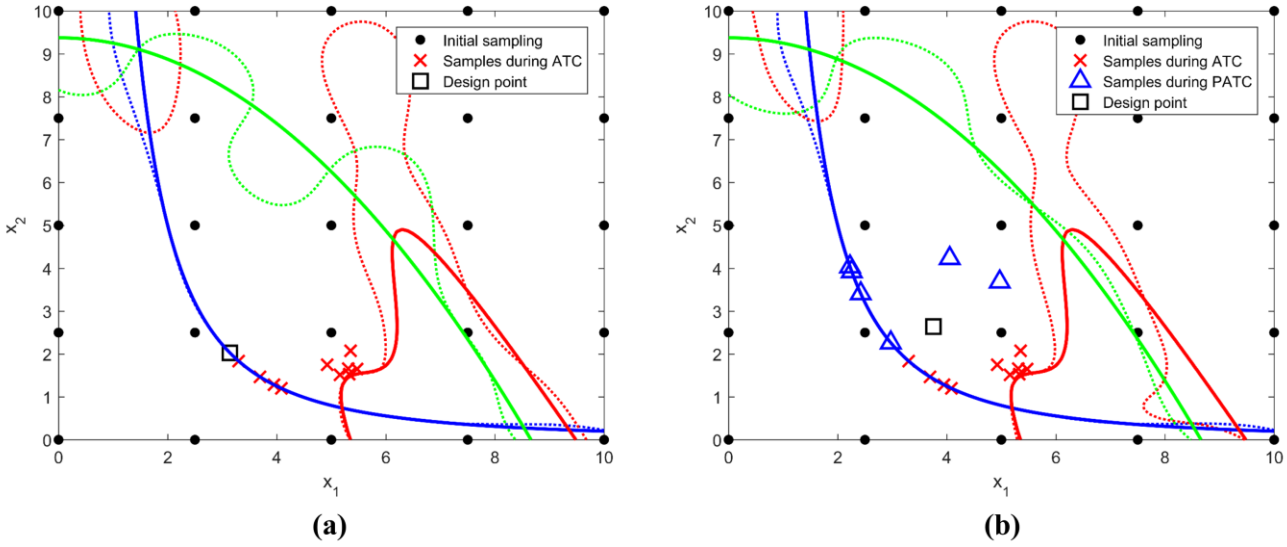

Fig. 8 Optimum and additional samples in the design space of Subsystem 1: (a) ATC (b) Sampling-based PATC

Table 4 Optimization results of the proposed sampling-based PATC

	Subsystem 1	Subsystem 2
Initial grid samples	25 (5^2)	25 (5^2)
Additional samples during ATC	10	2
Additional samples during PATC	6	6
Total samples	41	33
Mean of coupling variable	2.6056	2.6033
System optimum	$\{3.7550, 2.6438, 4.0323\}^T$	
Probability of failure (%)	[5.02, 4.95, 5.01]	

Table 5 Optimization results of PATC using moment-matching

	Results
Moments of coupling variable	$\mu = 2.6676$, $\sigma^2 = 0.7647$
System optimum	$\{3.7970, 2.5855, 4.0660\}^T$
Probability of failure (%)	[5.06, 3.89, 5.94]

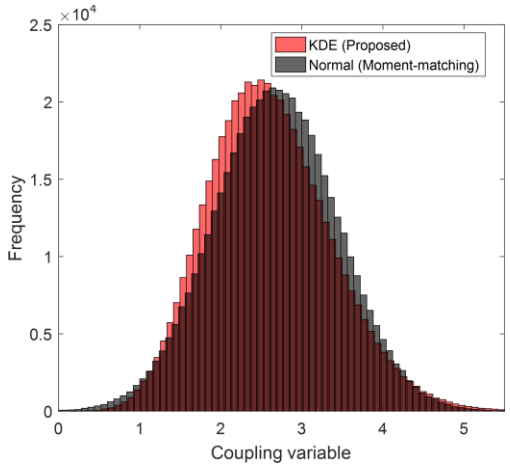

Fig. 9 Distribution of coupling variable in case of PATC with moment-matching and proposed PATC

5. Engineering Example: Roof Assembly Optimization

An engineering example incorporating FEA models is employed to verify feasibility of the proposed method in real complex engineering applications. This example is originated from the optimization of a bus body structure (Kang et al. 2014b) and modified by Jung et al. (2018) for simplification. In this paper, optimization of the components − cross-sections of beams − is refined to increase the number of design variables. There is a roof assembly optimization to satisfy displacement constraints with respect to the bending and torsion as shown in Figure 10 (a). On the other hand, the roof assembly consists of various types of the beams, and two types of I-beams used in the roof assembly shown in Figure 10 (b) are selected for optimization. Thus, there are six random design variables in each cross-section of the beam, and linking variables are the cross-sectional area and two perpendicular moments of inertia (MOI) of the cross-section described in Figure 11. In the roof optimization, the objective function is a penalty function for consistency constraints, and design variables are coupling variables that are MOI linked with each beam without any local and shared variable. In the optimization of beam, the objective function is mass and penalty function for consistency constraints, and there are only local variables to be optimized.

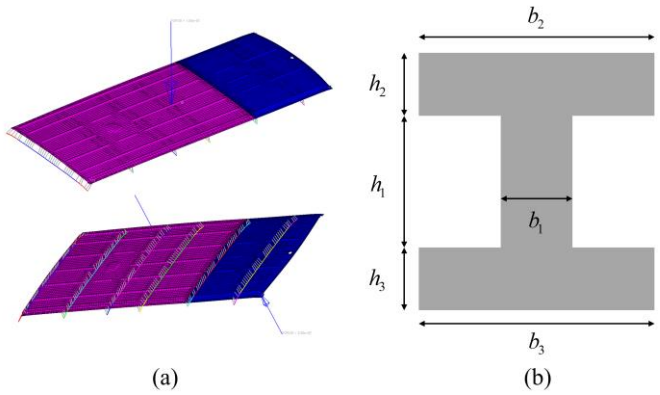

Fig. 10 (a) FEA model of a roof assembly including various beams and (b) design variables in the cross-section of I-beam

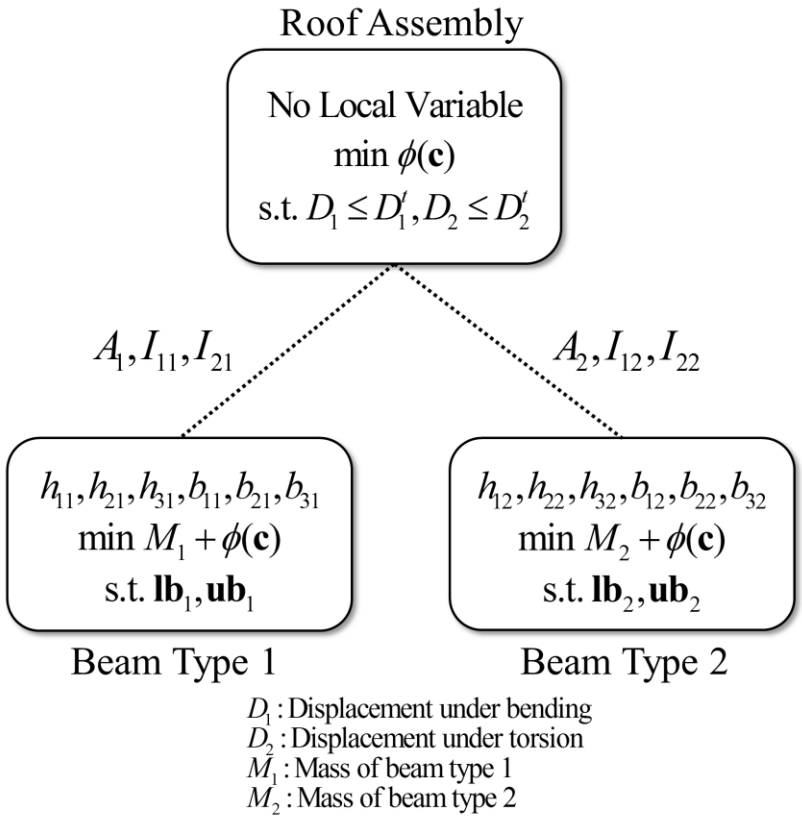

Fig. 11 Decomposition details for a roof assembly optimization with two types of beams

In conclusion, the original 12-dimensional RBDO problem is divided into three 6-dimensional RBDO problems linked with coupling variables. For a roof assembly, there are six coupling variables which are MOI of each beam, and the maximum displacements when a single force is exerted on the center of the structure (i.e., bending) and the given boundary node (i.e., torsion) are set to 74.5 mm and 450.5 mm, respectively. The target probability of failure is set to 5.00% for each constraint. The design space is defined in ±20% from the initial design variable. On the other hand, six design variables in each beam follow a normal distribution with coefficient of variation of 0.05. The objective is to reduce the beam mass only with boundary constraints described in Figure 11 which shows local design variables, objective function, inequality constraint functions, and equality constraint function from top to bottom in each box. Especially, in component-level optimization, the sequential sampling strategy and surrogate modeling are unnecessary since the coupling responses which are MOI of the cross-section can be computed in simple mathematical functions without FEA model. On the other hand, FEA model of a roof assembly is used to obtain displacements. Latin hypercube sampling (LHS) is used for initial sampling in 6-dimensional design space of the roof assembly.

Table 6 shows roof assembly optimization results by deterministic ATC and the proposed PATC. The deterministic ATC reduced the roof assembly mass by 16% satisfying two displacement constraints. Using the deterministic optimum as the initial design, the sampling-based PATC is performed to satisfy 95% reliability of two displacement constraints. From the table, it can be seen that the displacement constraint for torsion is active and the normalized mass is increased from 0.844 to 0.875 to guarantee reliability. It is noted that additional samples are not required since the surrogate model is already accurate enough with 150 LHS samples. This engineering example verifies the feasibility of the proposed sampling-based PATC.

Table 6 Roof assembly optimization results by deterministic ATC and proposed sampling-based PATC

	Initial	Deterministic	Proposed PATC
Roof assembly			
Normalized mass	1	0.844	0.875
Displacement for bending [mm]	74.121	74.155	74.152 (0.00%)
Displacement for torsion [mm]	450.339	450.49	450.29 (5.02%)

1st type beam			
h_1 [mm]	10.00	9.84	10.03
h_2 [mm]	5.00	4.00	4.00
h_3 [mm]	5.00	4.18	4.00
b_1 [mm]	5.00	4.00	4.00
b_2 [mm]	15.00	12.00	12.00
b_3 [mm]	15.00	18.00	17.99
2nd type beam			
h_1 [mm]	10.00	12.00	12.00
h_2 [mm]	5.00	4.57	5.56
h_3 [mm]	5.00	4.00	4.00
b_1 [mm]	5.00	4.00	4.00
b_2 [mm]	15.00	17.75	17.07
b_3 [mm]	15.00	12.00	12.00

6. Conclusion

This paper proposes sampling-based PATC using shifted KDE for uncertainty propagation between linked subsystems. The uncertainty propagation of linking variables – essential process to attain the consistency – is developed to deliver statistical information between linked subsystems utilizing KDE. Through the proposed method, individual optimization of subsystems incorporating uncertainty can yield a reliable optimum efficiently under the scheme of sampling-based RBDO, and uncertainty of coupling variables has been successfully treated employing stochastic sensitivity analysis for KDE. It means that the coupling variables propagated from coupling response of linked subsystems behave as random variables through resampling from shifted KDE and stochastic sensitivity analysis at the current design point. The proposed method is successfully applied to real engineering problems incorporating FEA. It is desirable to use surrogate models since PATC requires a large number of function evaluations with iterative optimizations. In this paper, constraints boundary sampling and Kriging model are used for the surrogate modeling of the bus roof assembly problem.

In future work, the dimension reduction effect of the proposed ATC will be further investigated. In previous works, it may be impractical to combine all subsystems into one due to complexity, and thus AiO is used only for comparison of accuracy rather than efficiency. However, a decomposed structure inherently contains several subsystems with reduced dimension which implies that the number of samples for accurate surrogate modeling

may decrease in the ATC framework compared with the high-dimensional AiO system. Hence, it will be further studied how to develop an efficient surrogate modeling based on the ATC framework which can be applied to solve large-scale & high dimensional engineering optimization problems by avoiding the curse of dimensionality.

7. Acknowledgements

This research was supported by the development of thermoelectric power generation system and business model utilizing non-use heat of industry funded by the Korea Institute of Energy Technology Evaluation and Planning (KETEP) and the Ministry of Trade Industry & Energy (MOTIE) of the Republic of Korea (No.20172010000830) and the National Research Foundation of Korea (NRF) grant funded by the Korean government (NRF-2017R1C1B2005266).

8. Replication of Results

Matlab codes for the three-dimensional mathematical example in Section 4 are uploaded on https://github.com/Yongsu-Jung/SMO_Submitted.git. Unfortunately, the engineering optimization is related to FEA models that are restricted so that it cannot be shared. Overall concepts and algorithms can be validated through the mathematical example.

9. Reference

Adhikari, S. (2004). Reliability analysis using parabolic failure surface approximation. *Journal of Engineering Mechanics*, 130(12), 1407-1427.

Alexandrov, N. M., & Lewis, R. M. (2002). Analytical and computational aspects of collaborative optimization for multidisciplinary design. *AIAA Journal*, 40(2), 301-309.

Allison, J. T., Kokkolaras, M., & Papalambros, P. Y. (2009). Optimal partitioning and coordination decisions in decomposition-based design optimization. *Journal of Mechanical Design*, 131(8), 081008.

Bae, S., Kim, N. H., & Jang, S. G. (2018). Reliability-based design optimization under sampling uncertainty: shifting design versus shaping uncertainty. *Structural and Multidisciplinary Optimization*, 57(5), 1845-1855.

Bayrak, A. E., Kang, N., & Papalambros, P. Y. (2016). Decomposition-based design optimization of hybrid electric powertrain architectures: Simultaneous configuration and sizing design. *Journal of Mechanical Design*, 138(7), 071405.

Breitung, K. (1984). Asymptotic approximations for multinormal integrals. *Journal of Engineering Mechanics*, 110(3), 357-366.

Chen, Y. C. (2017). A tutorial on kernel density estimation and recent advances. *Biostatistics & Epidemiology*, 1(1), 161-187.

Chen, Z., Qiu, H., Gao, L., Li, X., & Li, P. (2014). A local adaptive sampling method for reliability-based design optimization using Kriging model. *Structural and Multidisciplinary Optimization*, 49(3), 401-416.

Chen, Z., Peng, S., Li, X., Qiu, H., Xiong, H., Gao, L., & Li, P. (2015). An important boundary sampling method for reliability-based design optimization using kriging model. *Structural and Multidisciplinary Optimization*, 52(1), 55-70.

Cho, H., Bae, S., Choi, K. K., Lamb, D., & Yang, R. J. (2014). An efficient variable screening method for effective surrogate models for reliability-based design optimization. *Structural and Multidisciplinary Optimization*, 50(5), 717-738.

Cho, H., Choi, K. K., Lee, I., & Lamb, D. (2016). Design sensitivity method for sampling-based RBDO with varying standard deviation. *Journal of Mechanical Design*, 138(1), 011405.

Cho, S. G., Jang, J., Kim, S., Park, S., Lee, T. H., Lee, M., ... & Hong, S. (2016). Nonparametric approach for uncertainty-based multidisciplinary design optimization considering limited data. *Structural and Multidisciplinary Optimization*, 54(6), 1671-1688.

Denny, M. (2001). Introduction to importance sampling in rare-event simulations. *European Journal of Physics*, 22(4), 403.

DorMohammadi, S., & Rais-Rohani, M. (2013). Exponential penalty function formulation for multilevel optimization using the analytical target cascading framework. *Structural and Multidisciplinary Optimization*, 47(4), 599-612.

Du, X., & Chen, W. (2001). A most probable point-based method for efficient uncertainty analysis. Journal of Design and Manufacturing automation, 4(1), 47-66.

Du, X., & Chen, W. (2004). Sequential Optimization and Reliability Assessment Method for Efficient Probabilistic Design. *Journal of Mechanical Design*, 126(2), 225-233.

Dubourg, V., Sudret, B., & Bourinet, J. M. (2011). Reliability-based design optimization using kriging surrogates and subset simulation. *Structural and Multidisciplinary Optimization*, 44(5), 673-690.

Dubourg, V., Sudret, B., & Deheeger, F. (2013). Metamodel-based importance sampling for structural reliability analysis. *Probabilistic Engineering Mechanics*, 33, 47-57.

Han, J., & Papalambros, P. Y. (2010). A sequential linear programming coordination algorithm for analytical target cascading. *Journal of Mechanical Design*, 132(2), 021003.

Jung, Y., Kang, N., & Lee, I. (2018). Modified augmented Lagrangian coordination and alternating direction method of multipliers with parallelization in non-hierarchical analytical target cascading. *Structural and Multidisciplinary Optimization*, 58(2), 555-573.

Kang, N., Kokkolaras, M., & Papalambros, P. Y. (2014a). Solving multiobjective optimization problems using quasi-separable MDO formulations and analytical target cascading. *Structural and Multidisciplinary Optimization*, 50(5), 849-859.

Kang, N., Kokkolaras, M., Papalambros, P. Y., Yoo, S., Na, W., Park, J., & Featherman, D. (2014b). Optimal design of commercial vehicle systems using analytical target cascading. *Structural and Multidisciplinary Optimization*, 50(6), 1103-1114.

Kang, S. B., Park, J. W., & Lee, I. (2017). Accuracy improvement of the most probable point-based dimension reduction method using the hessian matrix. *International Journal for Numerical Methods in Engineering*, 111(3), 203-217.

Kim, H. M., Michelena, N. F., Papalambros, P. Y., & Jiang, T. (2003b). Target cascading in optimal system design. *Journal of Mechanical Design*, 125(3), 474-480.

Kim, H. M., Rideout, D. G., Papalambros, P. Y., & Stein, J. L. (2003a). Analytical target cascading in automotive vehicle design. *Journal of Mechanical Design*, 125(3), 481-489.

Kim, H. M., Chen, W., & Wiecek, M. M. (2006). Lagrangian coordination for enhancing the convergence of analytical target cascading. *AIAA Journal*, 44(10), 2197-2207.

Kokkolaras, M., Louca, L., Delagrammatikas, G., Michelena, N., Filipi, Z., Papalambros, P., ... & Assanis, D. (2004). Simulation-based optimal design of heavy trucks by model-based decomposition: An extensive analytical target cascading case study. *International Journal of Heavy Vehicle Systems*, 11(3-4), 403-433.

Kokkolaras, M., Mourelatos, Z. P., & Papalambros, P. Y. (2006). Design optimization of hierarchically decomposed multilevel systems under uncertainty. *Journal of Mechanical Design*, 128(2), 503-508.

Lee, I., Choi, K. K., Du, L., & Gorsich, D. (2008). Dimension reduction method for reliability-based robust design optimization. *Computers & Structures*, 86(13-14), 1550-1562.

Lee, I., Choi, K. K., & Zhao, L. (2011a). Sampling-based RBDO using the stochastic sensitivity analysis and Dynamic Kriging method. *Structural and Multidisciplinary Optimization*, 44(3), 299-317.

Lee, I., Choi, K. K., Noh, Y., Zhao, L., & Gorsich, D. (2011b). Sampling-based stochastic sensitivity analysis using score functions for RBDO problems with correlated random variables. *Journal of Mechanical Design,* 133(2), 021003.

Lee, I., Noh, Y., & Yoo, D. (2012). A novel second-order reliability method (SORM) using noncentral or generalized chi-squared distributions. *Journal of Mechanical Design,* 134(10), 100912.

Lee, T. H., & Jung, J. J. (2008). A sampling technique enhancing accuracy and efficiency of metamodel-based RBDO: Constraint boundary sampling. *Computers & Structures,* 86(13), 1463-1476.

Li, Y., Lu, Z., & Michalek, J. J. (2008). Diagonal quadratic approximation for parallelization of analytical target cascading. *Journal of Mechanical Design,* 130(5), 051402.

Lim, J., Lee, B., & Lee, I. (2014). Second-order reliability method-based inverse reliability analysis using Hessian update for accurate and efficient reliability-based design optimization. *International Journal for Numerical Methods in Engineering,* 100(10), 773-792.

Liu, H., Chen, W., Kokkolaras, M., Papalambros, P. Y., & Kim, H. M. (2006). Probabilistic analytical target cascading: a moment matching formulation for multilevel optimization under uncertainty. *Journal of Mechanical Design,* 128(4), 991-1000.

Liu, Y., Shi, Y., Zhou, Q., & Xiu, R. (2016). A sequential sampling strategy to improve the global fidelity of metamodels in multi-level system design. *Structural and Multidisciplinary Optimization,* 53(6), 1295-1313.

Martins, J. R., & Lambe, A. B. (2013). Multidisciplinary design optimization: a survey of architectures. *AIAA Journal,* 51(9), 2049-2075.

Michelena, N., Park, H., & Papalambros, P. Y. (2003). Convergence properties of analytical target cascading. *AIAA Journal,* 41(5), 897-905.

Ouyang, Q., Chen, X., & Yao, W. (2014). Sequential probabilistic analytical target cascading method for hierarchical multilevel optimization under uncertainty. *Structural and Multidisciplinary Optimization,* 49(2), 267-280.

Ouyang, Q., Yao, W., & Chen, X. (2018). Mixed uncertainty based analytical target cascading: an approach for hierarchical multilevel optimization under probabilistic and interval mixed uncertainties. *Structural and Multidisciplinary Optimization,* 57(4), 1475-1493.

Papalambros, P. Y., & Wilde, D. J. (2017). Principles of optimal design: modeling and computation. *Cambridge university press.*

Rubinstein, R. Y., & Kroese, D. P. (2016). Simulation and the Monte Carlo method (Vol. 10). *John Wiley & Sons.*

Silverman, B. W. (2018). Density estimation for statistics and data analysis. *Routledge.*

Sobieszczanski-Sobieski, J., & Haftka, R. T. (1997). Multidisciplinary aerospace design optimization: survey of recent developments. *Structural Optimization,* 14(1), 1-23.

Tosserams, S., Etman, L. F. P., Papalambros, P. Y., & Rooda, J. E. (2006). An augmented Lagrangian relaxation for analytical target cascading using the alternating direction method of multipliers. *Structural and Multidisciplinary Optimization,* 31(3), 176-189.

Tosserams, S., Etman, L. F. P., & Rooda, J. E. (2008). Augmented Lagrangian coordination for distributed optimal design in MDO. *International Journal for Numerical Methods in Engineering,* 73(13), 1885-1910.

Tosserams, S., Kokkolaras, M., Etman, L. F. P., & Rooda, J. E. (2010). A nonhierarchical formulation of analytical target cascading. *Journal of Mechanical Design,* 132(5), 051002.

Tu, J., Choi, K. K., & Park, Y. H. (1999). A new study on reliability-based design optimization. *Journal of Mechanical Design,* 121(4), 557-564.

Xiong, F., Yin, X., Chen, W., & Yang, S. (2010). Enhanced probabilistic analytical target cascading with application to multi-scale design. *Engineering Optimization,* 42(6), 581-592.

Yao, W., Chen, X., Luo, W., van Tooren, M., & Guo, J. (2011). Review of uncertainty-based multidisciplinary design optimization methods for aerospace vehicles. *Progress in Aerospace Sciences,* 47(6), 450-479.

Zhao, L., Choi, K. K., & Lee, I. (2011). Metamodeling method using dynamic kriging for design optimization. *AIAA Journal,* 49(9), 2034-2046.